RESEARCH PAPER

Photocatalytic Degradation of Rhodamine B, and Phenol Red Dyes using $NiMn_2O_4$ Nanoparticles Prepared by a New Approach

Farideh Sedighi [1], *Ali Sobhani-Nasab* [2,3]*, *Mohsen Behpour* [1], *Mehdi Rahimi-Nasrabadi* [4,5]

[1] Institute of Nano Science and Nano Technology, University of Kashan, Kashan, Iran

[2] Social Determinants of Health (SDH) Research Center, Kashan University of Medical Sciences, Kashan, Iran

[3] Core Research Lab, Kashan University of Medical Sciences, Kashan, Iran

[4] Nanobiotechnology Research Center, Baqiyatallah University of Medical Sciences, Tehran, Iran

[5] Faculty of Pharmacy, Baqiyatallah University of Medical Sciences, Tehran, Iran

ARTICLE INFO

Article History:
Received 06 December 2018
Accepted 22 February 2019
Published 01 April 2019

Keywords:
Amino acid
Nanostructure
New approach
$NiMn_2O_4$
Photocatalyst

ABSTRACT

$NiMn_2O_4$ nanoparticles have been successfully prepared through sol-gel method. The effects of different factors such as the type of solvent, and amino acid temperature were investigated on the size and morphologies of products. The smallest particle size of $NiMn_2O_4$ nanoparticles was found to be 25 nm in diameter. The magnetic properties of the samples were also measured by an alternating gradient force magnetometer (AGFM). The optical property of the desired products was investigated by UV–vis diffuse reflectance spectroscopy, and the band gap of product was computed nearly 3 eV. The estimated band gap confirms that this product may be used as a photocatalyst, so the photocatalytic test was conducted by photooxidation of dyes under ultraviolet irradiation and in the presence of $NiMn_2O_4$ nanoparricles. The results demonstrated that rhodamine B degradation was about 98 % under ultraviolet light for 80 min. Therefore, the synthesized product can be employed as an effective photocatalyst.

How to cite this article
Sedighi F, Sobhani-Nasab A, Behpour M, Rahimi-Nasrabadi M. Photocatalytic Degradation of Rhodamine B, and Phenol Red Dyes using $NiMn_2O_4$ Nanoparticles Prepared by a New Approach. J Nanostruct, 2019; 9(2): 258-267.
DOI: 10.22052/JNS.2019.02.008

INTRODUCTION

Turning materials from bulk into nanostructure can have interesting outcome which is substantial changes in their physical properties. From structural point of view, it has been demonstrated that bulk material which have molecular structure of AB_2O_4 show a normal spinel-type structure which is a very famous structure and various ions can flexibly incorporate into their crystal structure. In this structure, atoms A(divalent cations) and B (trivalent cations) take up one-eighths of tetrahedral and half of octahedral sites, respectively. These atoms are distributed to fcc lattice constituted by the O^{2-} ions [1]. Undergoing some procedures such as mixed spinel or inverse spinel structure, may alter their crystal structure in a way that B^{3+} occupies both the tetrahedral and the octahedral sites and the A^{2+} ions occupy octahedral ones. Moreover, in materials with general formula of $(A_{1\_x} B_x)$ $[A_x B_{2\_x}]$ O_4, mixed spinel structures, A and B atoms can take up both octahedral and tetrahedral sites [2]. Among numerous materials with spinel structure, $NiMn_2O_4$ has gained much attention, Because catalytic activities and electrical resistance of the $NiMn_2O_4$ are highly dependent on the temperature [3, 4]. This feature has motivated researchers in synthesis of $NiMn_2O_4$. However, in most methods of synthesis, prolong time and high temperature which are the necessary steps to sinter, make those procedures inappropriate for production of this compound [5, 6].

J. M. A. Almeida and co-worker synthesized $NiMn_2O_4$ by gelatin, as an organic precursor and the average crystalline size of nanoscaled

* Corresponding Author Email: ali.sobhaninasab@gmail.com

$NiMn_2O_4$ was found to be in the range of 14-44 nm. Also, they discovered that both unit cell parameters and average crystallite size are positively correlated with synthesis temperature and magnetic transition occurred in 110 K [8]. In this work, we synthesized $NiMn_2O_4$ nanostructure by new approach. Besides, several experiments were performed in order to investigate the effect of different solvents and capping agents such as valine, asparagine and arginine on the morphology, particle size, and crystal structure of final products. The photocatalytic activities of $NiMn_2O_4$ catalysts were studied for the degradation of methyl orange under ultraviolet light [9-16].

MATERIALS AND METHODS

Synthesis of $NiMn_2O_4$ nanoparticles

$NiMn_2O_4$ nanoparticles were prepared using sol-gel method. First, capping agents solution was added dropwise into the nickel chloride solution under magnetic stirrer and then manganese nitrate solution was added into the above solution (with molar ratio of Mn:Ni = 2:1). The pH of solution was regulated to 4-5. The gained green gel was dried at temperature 100 for 5 h. The as-obtained products were dried at 100 ˚C under vacuum for 3 h. Next, these products were calcined at 700 ˚C and 800 ˚C for 2 h. The preparation conditions of $NiMn_2O_4$ nanoparticles have been depicted in Table 1.

Photocatalytic test

The photocatalytic activity of nanoscaled $NiMn_2O_4$ was investigated by rhodamine B (Rh B), and phenol red (Ph R) solution. The degradation reaction was conducted in a quartz photocatalytic reactor. The photocatalytic degradation was conducted with 5×10^{-5} M of solutions containing 0.05 g of nanoparticles. Then in order to reach adsorption equilibrium the mixture was aerated for 30 min. Then, the mixture was placed in the photoreactor in which the vessel was nearly 30 cm away from the UV source. A 400W ultraviolet light lamp was used as a visible light source, and the experiments were performed at room temperature. Furthermore, the pH of the solutions were adjusted to 3. The mixture was aliquoted in periodic intervals throughout the irradiation, and before the analysis of mixture with the UV–Vis spectrometer, it was centrifuged. The percentage of dyes degradation was appraised as the following formula.

$$\text{Degradation rate (\%)} = 100\,(C_0 - C_t) / C_0 \qquad (1)$$

Where C_0 and C_t are the absorbance value of solution at 0 and t min, respectively.

Materials and physical measurements

$Mn(NO_3)_3{\cdot}9H_2O$, $NiCl_2$, valine, asparagine and arginine was purchased from Merck and all the chemicals were used as received without further purifications. Room temperature magnetic properties were investigated using an alternating gradient force magnetometer (AGFM) device, (made by Meghnatis Daghigh Kavir Company, Iran) in an applied magnetic field sweeping between ± 10000 Oe. XRD patterns were recorded by a Philips, X-ray diffractometer using Ni-filtered Cu Kα radiation. SEM images were obtained using a LEO instrument model 1455VP. Prior to taking images, the samples were coated by a very thin layer of Pt (using a BAL-TEC SCD 005 sputter coater) to make the sample surface conductor and prevent charge accumulation, and obtaining a better contrast. An S-10 4100 Scinco UV-Vis scanning spectrometer was used to obtain the electronic spectra.

RESULTS AND DISCUSSION

A lot of interest has recently expressed toward controlling the particle size and shape of the nanostructures by manipulating reaction parameters [17–23]. As a result, several experiments were performed to verify the influences of the presence of natural polymers on the size and morphology of the nanostructures.

Fig 1a-c represents as-prepared $NiMn_2O_4$ nanoparticles with glycerol, 2-propanol, and water in the presence of valin as a capping agent respectively. As this figure demonstrates, by changing the solvent from glycerol (Fig. 1a) to propanol (Fig. 1b), and then to water (Fig. 1c)

Table 1. Preparation conditions for the synthesis of $NiMn_2O_4$ nanoparticles.

Sample No	Solvent	Capping agent	Decolorization(%) Ph R	Decolorization(%) Rh B
1	glycerin	valine	-	-
2	2-Propanol	valine	-	-
3	Water	valine	-	-
4	Water	asparagine	-	-
5	Water	arginine	65	98

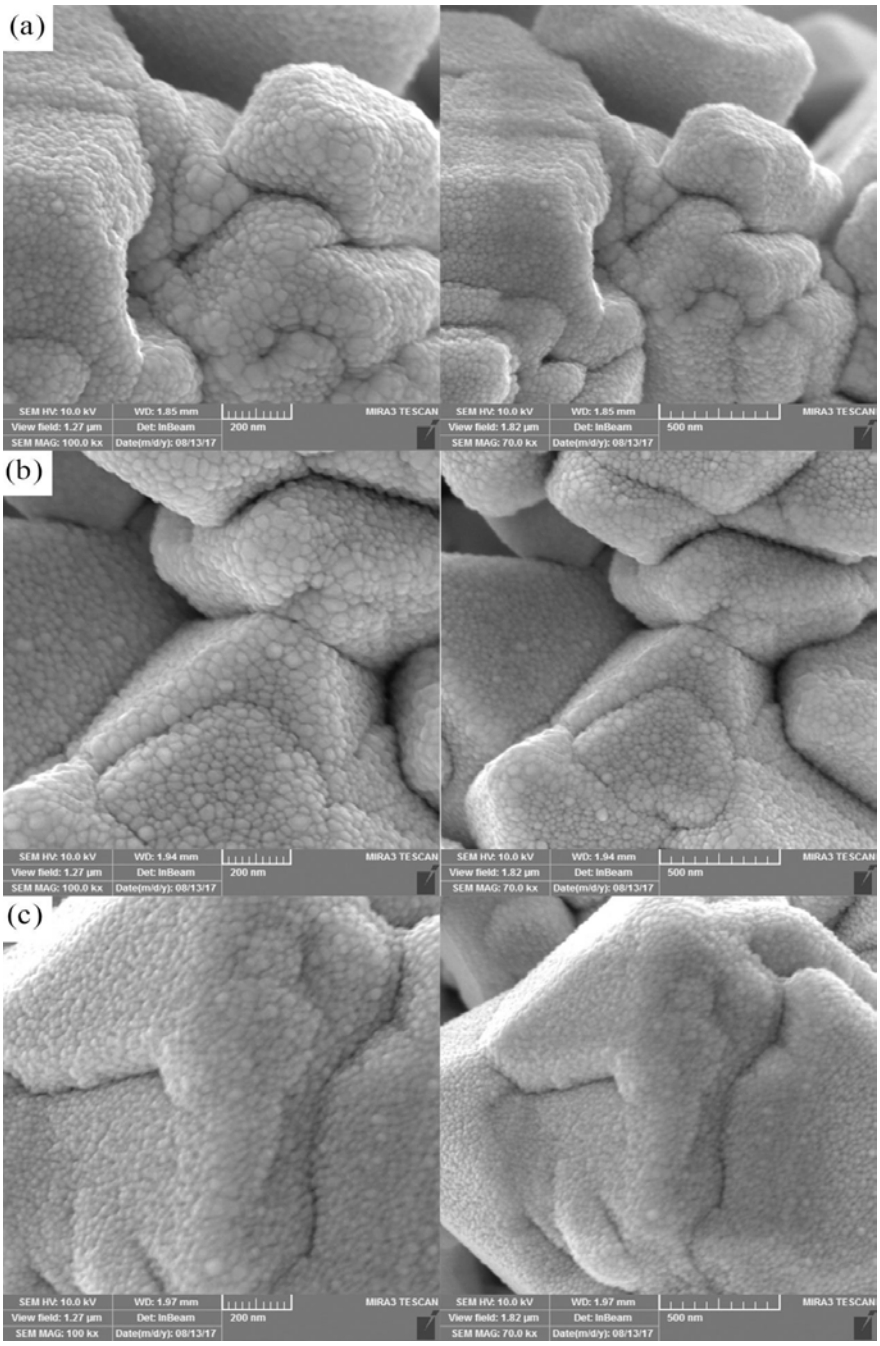

Fig. 1. SEM images of $NiMn_2O_4$ nanoparticles obtained with various solvents of a) glycerin, b) 2-Propanol, and c) water

the size of final products was reduced. The effect of amino acids such as asparagine and arginine on the morphology and particle size of $NiMn_2O_4$ nanoparticles has been investigated in Fig. 2 a and b. As shown in the figure, increasing steric hinderance in amino acids leads to smaller particle size (Fig. 3).

The crystalline structure and phase of $NiMn_2O_4$ nanoparticles were verified by the XRD analysis. Fig. 4 and Fig. 5 illustrtes the XRD patterns of products prepared at 700 ˚C and 800 ˚C respectively. The peak intensity of $NiMn_2O_4$ increases through

enhancing the calcinations temperature, and the broadening of peaks decreases owing to growth of the nanoparticles.

The crystallite size of the products (D) can be computed from XRD patterns by Scherrer's equation [24]:

$$D = 0.9\lambda/FWHM \cos(\theta); \quad (2)$$

Where λ is the wavelength of incident X-rays, FWHM is full width at half maximum and θ is the position of the maximum of the diffraction peak. The average crystallite size of the products was evaluated about 9/3 and 7/1 nm, correspondingly.

EDS analysis proves presence of Ni, Mn, and O elements without any impurity (Fig. 6). The magnetization measurements as a function of the magnetic field were evaluated at 300 K. Also, the hysteric curve with nearly saturated nature at high fields has been shown in Fig. 7. The magnetic property of $NiMn_2O_4$ nanoparticles was obtained at room temperature. VSM analysis shows that $NiMn_2O_4$ nanoparticles have ferromagnetic properties. The saturation magnetization and coercivity are found 0.3 emu/g.

It is famous that the band-gap of the nanostructures materials has a major role in utilizing photocatalytic applications. The diffuse reflectance spectroscopy (DRS) of $NiMn_2O_4$ nanoparticles has been depicted in Fig. 8. The band-gap of the samples was calculated by the following equation (3) [25]:

$$(\alpha h\upsilon)^n = A\,(h\upsilon - E_g) \quad (3)$$

Where E_g is the optical band gap of the material, hυ is the photon energy, A is a material constant, α is the amount of the absorbance, and n is constant that depends on the type of the electronic transition [21]. The energy gap of the samples (E_g)

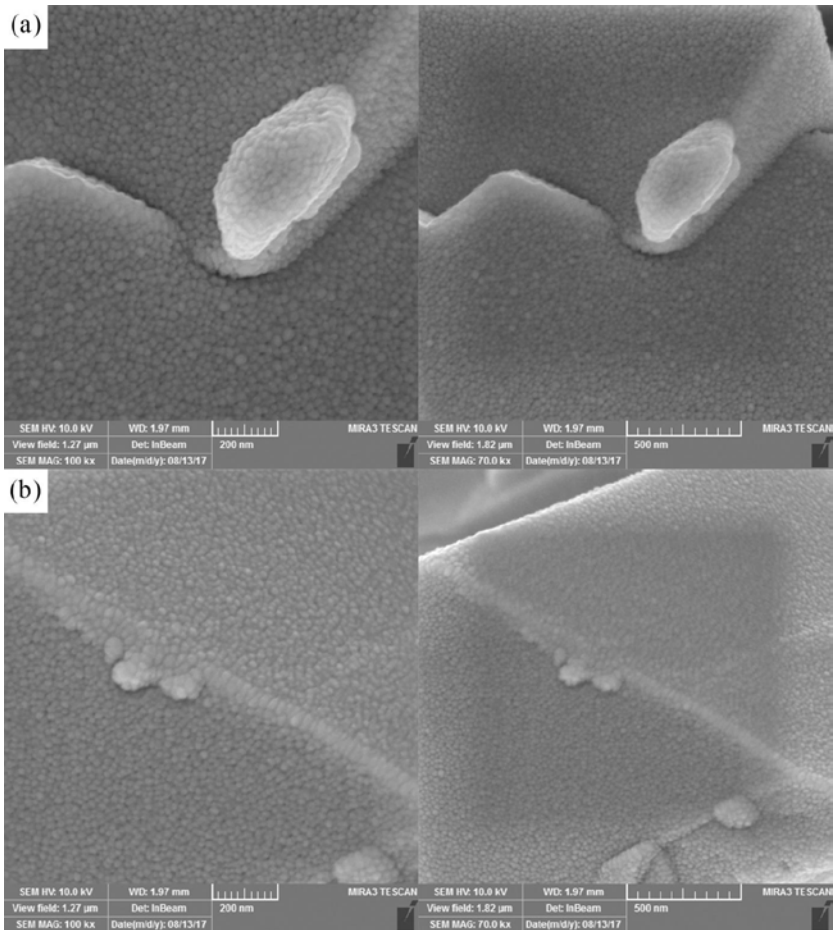

Fig. 2. SEM images of $NiMn_2O_4$ nanoparticles obtained with various capping agents of a) valine, b) asparagine, and c) arginine

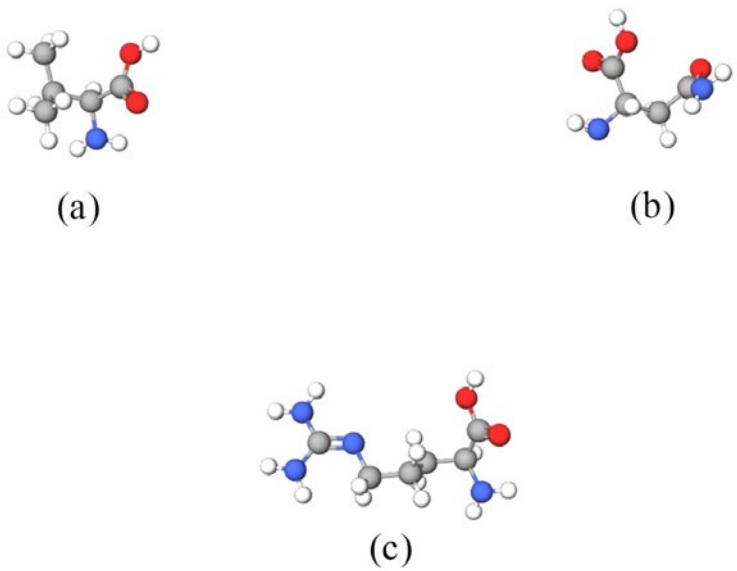

Fig. 3. Various amino acids used as capping agents such as (a) valine, (b) asparagine and *(c) arginine*.

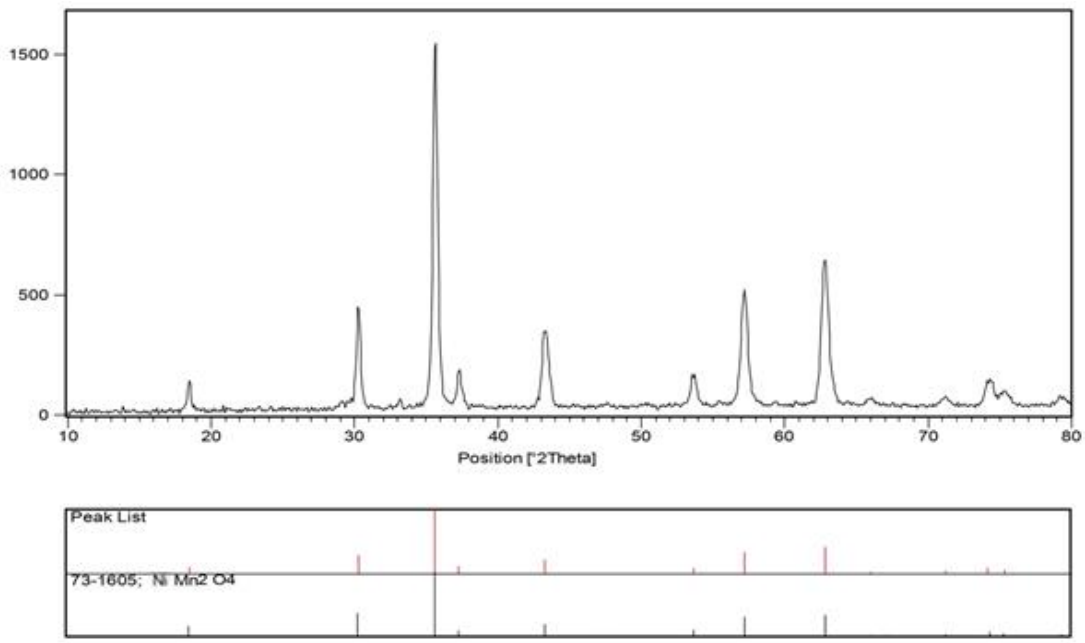

Fig. 4. XRD pattern of of $NiMn_2O_4$ nanoparticles obtained with arginine calcined at 700°C (sample No. 5)

was obtained by extrapolating the linear portion of the plots of $(\alpha h\upsilon)^2$ curve in return $h\upsilon$ to the energy axis. The band-gap (E_g) of $NiMn_2O_4$ nanoparticles were 3 eV.

The degradation rate of two different dyes such as rhodamine B (Rh B), and phenol red (Ph R) as organic pollutants was verified by $NiMn_2O_4$ nanoparticles under ultra violet. It is obvious that in Fig. 9 the photocatalytic activity of nanocomposite in decolouration of Rh B is higher than others as Photocatalytic efficience for Rh B and Ph R are 98%, and 65%, correspondingly.

Moreover, a photocatalytic test as a blank for the investigation of photacatalytic activity of $NiMn_2O_4$ nanoparticles was conducted. In this test degradation rate for rhodamine B (Rh B),

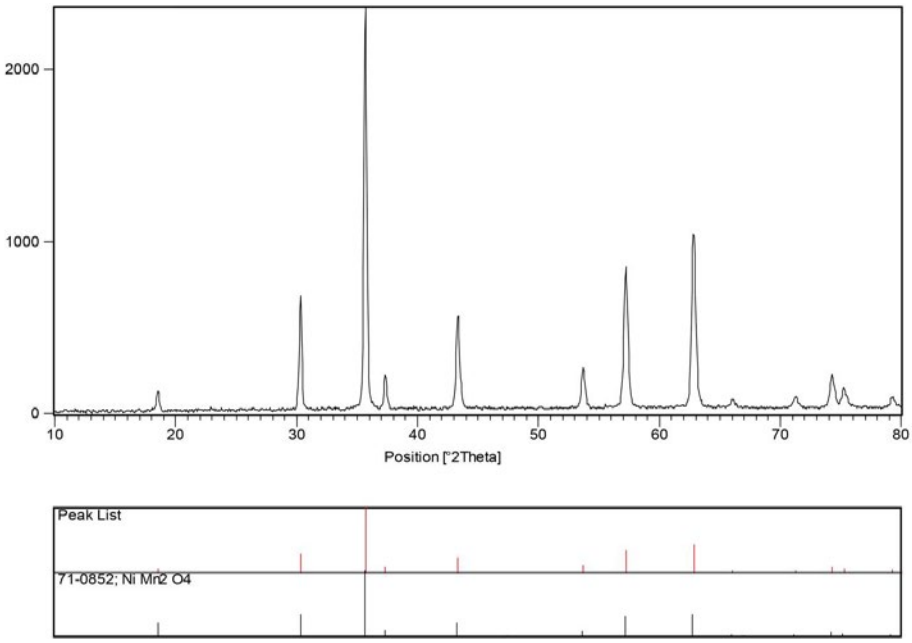

Fig. 5. XRD pattern of of $NiMn_2O_4$ nanoparticles obtained with arginine calcined at 800°C (sample No. 5)

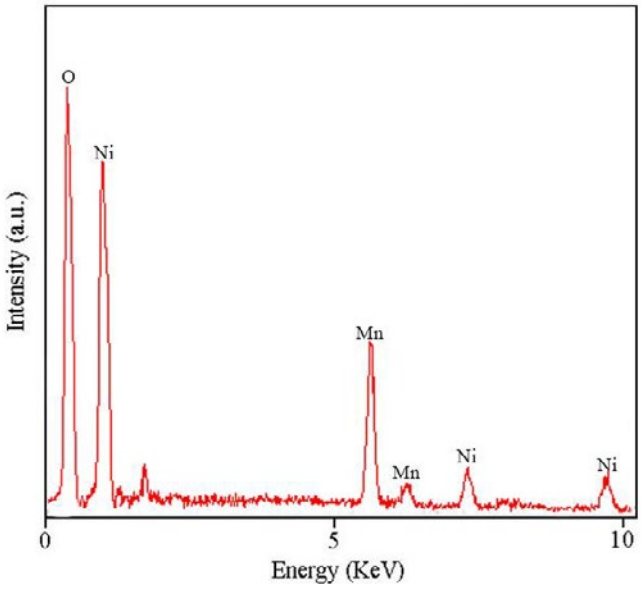

Fig. 6. EDS pattern of $NiMn_2O_4$ nanoparticles obtained with arginine calcined at 700°C (sample No. 5)

and phenol red (Ph R) was obtained 6% and 4% respectively. As illustrated, all three patterns confirm the presence of $NiMn_2O_4$ nanoparticles in the products.

The suggested procedure of photocatalytic degradation of Rh B can be as following:

$$NiMn_2O_4 + h\nu \rightarrow NiMn_2O_4^{\bullet} + e^- + h^+ \quad (4)$$

$$e^- + O_2 \rightarrow O_2^{\bullet -} \quad (5)$$

$$O_2^{\bullet -} + H_2O \rightarrow OOH^{\bullet} + OH^- \quad (6)$$

$$OOH^{\bullet} \rightarrow O_2 + H_2O_2 \quad (7)$$

$$H_2O_2 + O_2^{\bullet -} \rightarrow OOH^{\bullet} + OH^- + O_2 \quad (8)$$

$$OH^{\bullet} + \text{methyl orange} \rightarrow \text{Degradation products} \quad (9)$$

$$h^+ + \text{methyl orange} \rightarrow \text{degradation products} \quad (10)$$

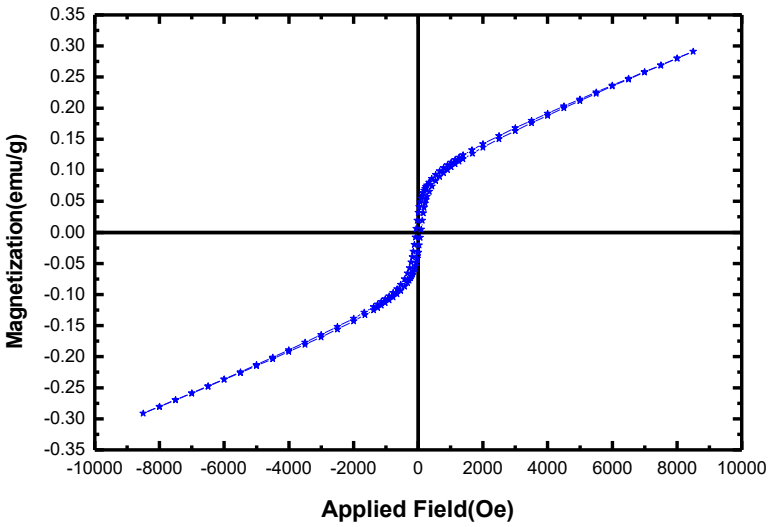

Fig. 7. VSM curves of $NiMn_2O_4$ nanoparticles obtained with arginine calcined at 700°C (sample No. 5)

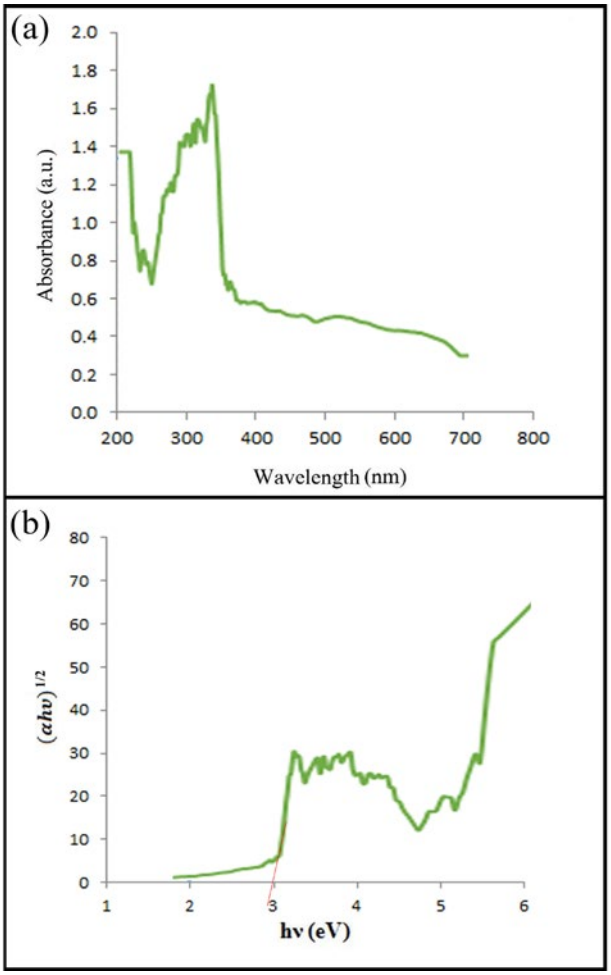

.Fig. 8. UV–vis diffuse reflectance spectrum (a) of the asprepared of $NiMn_2O_4$ nanoparticles and Tauc plot pattern of $NiMn_2O_4$ nanoparticles (sample No. 5)

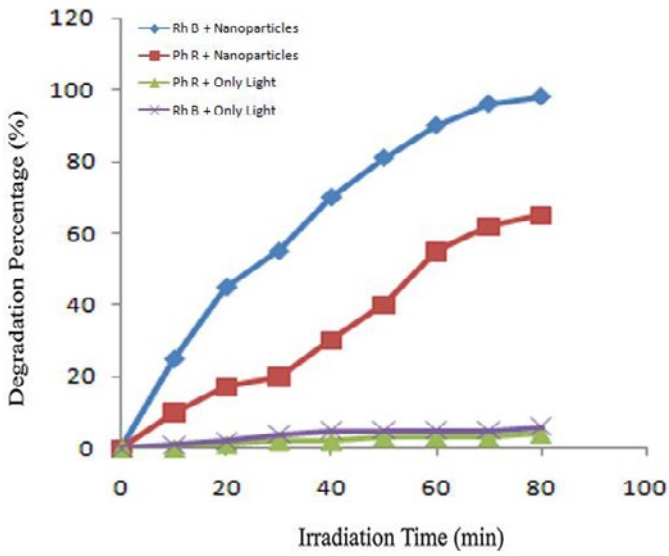

Fig. 9. The photocatalytic behavior of $NiMn_2O_4$ nanoparticles calcined at 700 °C (sample No. 5) on decomposition of various contaminants (cationic and anionic types)

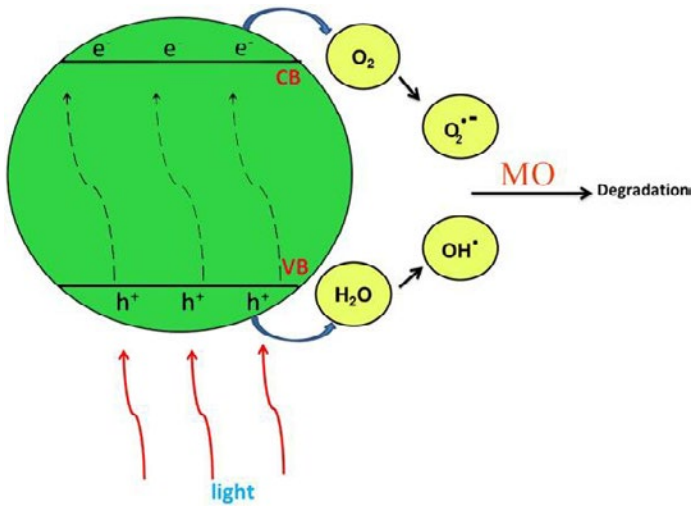

Fig. 10. Reaction mechanism of dyes photodegradation over $NiMn_2O_4$ nanoparticles under UV light irradiation.

The composition procedure of contaminants for the $NiMn_2O_4$ nanoparticles has been depicted in Fig. 10. These consequences show a high degree of competence of the as-produced $NiMn_2O_4$ nanoparticles (sample No. 5) to be employed as an appropriate, new, and favorable type of photocatalyst under ultraviolet light for elimination of cationic contaminants. Moreover, applying of polymers as capping gents for production of nanocomposites is the creativity of this effort. Moreover, changing the capping agent resulted in production of a fine grain size and very homogenous and sphere-like $NiMn_2O_4$ nanoparticles. Interestingly, to the best of our knowledge, in the literature, there is no report on the study of photocatalytic activity of $NiMn_2O_4$ nanoparticles. Further, photocatalytic activity of final products can be influenced by various factors such as grain size of $NiMn_2O_4$ nanoparticles and kind of pollutant. The outcomes demonstrated that the as-prepared $NiMn_2O_4$ nanoparticles show considerable possibility to be used as a proper, useful, and innovative kind of photocatalyst under visible light to erase cationic contaminants.

Respecting the production of $NiMn_2O_4$ nanoparticles, one can simply understand the facileness, convenience, and originality of the approach stated above [26-28]. In comparison to other similar works illustrated in Table 2, our method is simple, has low cost, and scale-up route. Besides, to the best of author's knowledge, it is the first time that $CuMn_2O_4$ nanoparticles was synthesized in the presence of amino acids as the capping agent and used for degradation of rhodamine B, and phenol red under ultraviolet light.

CONCLUSIONS

$NiMn_2O_4$ nanoparticles is prepared to remove dyes from water. Furthermore, the evaluated band gap of $NiMn_2O_4$ nanoparticles proves that it can be employed as a photocatalyst. In order to investigate the effect of several capping agents on the morphology and particle size of final products several tests were conducted in the presence of valine, asparagine and arginine. Applying nanocrystalline $NiMn_2O_4$ as the photocatalyst, causes maximum of 98 % for degradation of Rh B after 80 min irradiation under UV light. This result suggests that as-obtained nanocrystalline $NiMn_2O_4$ as favorable material has high potential to be used for photocatalytic applications under ultraviolet light. Furthermore, high purity of the as-prepared $NiMn_2O_4$ nanoparticles was proved by EDS and XRD analyses.

ACKNOWLEDGMENT

Authors are grateful to council of University of Kashan for providing financial support to undertake this work.

CONFLICT OF INTEREST

The authors declare that there are no conflicts of interest regarding the publication of this manuscript.

REFERENCES

1. Åsbrink S, Waśkowska A, Olsen JS, Gerward L. High-pressure phase of the cubic spinelNiMn2O4. Physical Review B. 1998;57(9):4972-4.
2. Lisboa-Filho PN, Vila C, Góes MS, Morilla-Santos C, Gama L, Longo E, et al. Composition and electronic structure of Zn7−xMxSb2O12 (M=Ni and Co) spinel compounds. Materials Chemistry and Physics. 2004;85(2-3):377-82.
3. Mehandjiev D, Naydenov A, Ivanov G. Ozone decomposition, benzene and CO oxidation over NiMnO3-ilmenite and NiMn2O4-spinel catalysts. Applied Catalysis A: General. 2001;206(1):13-8.
4. Schmidt R, Brinkman AW. Preparation and characterisation of NiMn2O4 films. International Journal of Inorganic Materials. 2001;3(8):1215-7.
5. Ashcroft G, Terry I, Gover R. Study of the preparation conditions for NiMn2O4 grown from hydroxide precursors. Journal of the European Ceramic Society. 2006;26(6):901-8.
6. Shen Y, Nakayama T, Arai M, Yanagisawa O, Izumi M. Magnetic phase transition and physical properties of spinel-type nickel manganese oxide. Journal of Physics and Chemistry of Solids. 2002;63(6-8):947-50.
7. Khademolhoseini S. Synthesis, characterization, and morphological control of nickel manganite nanoparticles through new method and its photocatalyst application. Journal of Materials Science: Materials in Electronics. 2017;28(11):7899-904.
8. Almeida JMA, Meneses CT, de Menezes AS, Jardim RF, Sasaki JM. Synthesis and characterization of NiMn2O4 nanoparticles using gelatin as organic precursor. Journal of Magnetism and Magnetic Materials. 2008;320(14):e304-e7.
9. Rahimi-Nasrabadi M. Effects of amino acid capping-agents on the size and morphology and photocatalytic properties of BNCTO nanostructures. Journal of Materials Science: Materials in Electronics. 2017;28(9):6373-8.
10. Hosseinpour-Mashkani SM, Sobhani-Nasab A. A simple sonochemical synthesis and characterization of CdWO4 nanoparticles and its photocatalytic application. Journal of Materials Science: Materials in Electronics. 2015;27(4):3240-4.
11. Eghbali-Arani M, Sobhani-Nasab A, Rahimi-Nasrabadi M, Ahmadi F, Pourmasoud S. Ultrasound-assisted synthesis of YbVO4 nanostructure and YbVO4/CuWO4 nanocomposites for enhanced photocatalytic degradation of organic dyes under visible light. Ultrasonics Sonochemistry. 2018;43:120-35.
12. Pourmasoud S, Sobhani-Nasab A, Behpour M, Rahimi-Nasrabadi M, Ahmadi F. Investigation of optical properties and the photocatalytic activity of synthesized YbYO4 nanoparticles and YbVO4/NiWO4 nanocomposites by polymeric capping agents. Journal of Molecular Structure. 2018;1157:607-15.
13. Salavati-Niasari M, Soofivand F, Sobhani-Nasab A, Shakouri-Arani M, Hamadanian M, Bagheri S. Facile synthesis and characterization of CdTiO3 nanoparticles by Pechini sol–gel method. Journal of Materials Science: Materials in Electronics. 2017;28(20):14965-73.
14. Hosseinpour-Mashkani SS, Sobhani-Nasab A. Investigation the effect of temperature and polymeric capping agents on the size and photocatalytic properties of NdVO4 nanoparticles. Journal of Materials Science: Materials in Electronics. 2017;28(21):16459-66.
15. Sobhani-Nasab A, Sadeghi M. Preparation and characterization of calcium tungstate nanoparticles with the aid of amino acids and investigation its photocatalytic application. Journal of Materials Science: Materials in Electronics. 2016;27(8):7933-8.
16. Ahmadi F, Rahimi-Nasrabadi M, Behpour M, Ganjali MR. A simple process for the preparation of photocatalytically active bismuth aluminate nanoparticles. Journal of Materials Science: Materials in Electronics. 2017;29(1):146-52.
17. Hosseinpour-Mashkani SM, Maddahfar M, Sobhani-Nasab A. Precipitation Synthesis, Characterization,

Morphological Control, and Photocatalyst Application of ZnWO4 Nanoparticles. Journal of Electronic Materials. 2016;45(7):3612-20.
18. Sobhani-Nasab A, Hosseinpour-Mashkani SM, Salavati-Niasari M, Bagheri S. Controlled Synthesis of CoTiO3 Nanostructures Via Two-Step Sol–Gel Method in the Presence of 1,3,5-Benzenetricarboxylic Acid. Journal of Cluster Science. 2014;26(4):1305-18.
19. Sobhani-Nasab A, Hosseinpour-Mashkani SM, Salavati-Niasari M, Taqriri H, Bagheri S, Saberyan K. Synthesis, characterization, and photovoltaic application of NiTiO3 nanostructures via two-step sol–gel method. Journal of Materials Science: Materials in Electronics. 2015;26(8):5735-42.
20. Sobhani-Nasab A, Zahraei Z, Akbari M, Maddahfar M, Hosseinpour-Mashkani SM. Synthesis, characterization, and antibacterial activities of ZnLaFe 2 O 4 /NiTiO 3 nanocomposite. Journal of Molecular Structure. 2017;1139:430-5.
21. Sobhani-Nasab A, Rahimi-Nasrabadi M, Naderi HR, Pourmohamadian V, Ahmadi F, Ganjali MR, et al. Sonochemical synthesis of terbium tungstate for developing high power supercapacitors with enhanced energy densities. Ultrasonics Sonochemistry. 2018;45:189-96.
22. Sobhani-Nasab A, Naderi H, Rahimi-Nasrabadi M, Ganjali MR. Evaluation of supercapacitive behavior of samarium tungstate nanoparticles synthesized via sonochemical method. Journal of Materials Science: Materials in Electronics. 2017;28(12):8588-95.
23. Salavati-Niasari M, Soofivand F, Sobhani-Nasab A, Shakouri-Arani M, Yeganeh Faal A, Bagheri S. Synthesis, characterization, and morphological control of ZnTiO3 nanoparticles through sol-gel processes and its photocatalyst application. Advanced Powder Technology. 2016;27(5):2066-75.
24. Ziarati A, Sobhani-Nasab A, Rahimi-Nasrabadi M, Ganjali MR, Badiei A. Sonication method synergism with rare earth based nanocatalyst: preparation of NiFe 2– x Eu x O 4 nanostructures and its catalytic applications for the synthesis of benzimidazoles, benzoxazoles, and benzothiazoles under ultrasonic irradiation. Journal of Rare Earths. 2017;35(4):374-81.
25. Mostafa Hosseinpour-Mashkani S, Maddahfar M, Sobhani-Nasab A. Novel silver-doped NiTiO3: auto-combustion synthesis, characterization and photovoltaic measurements. South African Journal of Chemistry. 2017(70).
26. Pourmasoud S, Eghbali-Arani M, Ahmadi F, Rahimi-Nasrabadi M. Synthesis, characterization, and morphological control of PbWO4 nanostructures through precipitation method and its photocatalyst application. Journal of Materials Science: Materials in Electronics. 2017;28(22):17089-97.
27. Hosseinpour-Mashkani SM, Sobhani-Nasab A. Green synthesis and characterization of NaEuTi2O6 nanoparticles and its photocatalyst application. Journal of Materials Science: Materials in Electronics. 2016;28(5):4345-50.
28. Hosseinpour-mashkani SM, Sobhani-Nasab A, Mehrzad M. Controlling the synthesis SrMoO4 nanostructures and investigation its photocatalyst application. Journal of Materials Science: Materials in Electronics. 2016;27(6):5758-63.
29. Hosseini SA, Niaei A, Salari D, Nabavi SR. Nanocrystalline AMn2O4 (A=Co, Ni, Cu) spinels for remediation of volatile organic compounds—synthesis, characterization and catalytic performance. Ceramics International. 2012;38(2):1655-61.
30. Sahoo S, Zhang S, Shim J-J. Porous Ternary High Performance Supercapacitor Electrode Based on Reduced Graphene Oxide, NiMn 2 O 4 , and Polyaniline. Electrochimica Acta. 2016;216:386-96.
31. Tadic M, Savic SM, Jaglicic Z, Vojisavljevic K, Radojkovic A, Prsic S, et al. Magnetic properties of NiMn2O4−δ (nickel manganite): Multiple magnetic phase transitions and exchange bias effect. Journal of Alloys and Compounds. 2014;588:465-9.